REGULAR ARTICLE

blood advances

# Endoplasmic reticulum protein 5 attenuates platelet endoplasmic reticulum stress and secretion in a mouse model

Angelina J. Lay,[1-3,*] Alexander Dupuy,[1,4,*] Lejla Hagimola,[1,3] Jessica Tieng,[1-3] Mark Larance,[5] Yunwei Zhang,[6] Jean Yang,[6] Yvonne Kong,[1,4] Joyce Chiu,[2,3] Emilia Gray,[1,3] Zihao Qin,[1,4] Diana Schmidt,[1,3] Jessica Maclean,[3,7] Benjamin Hofma,[3,7] Marc Ellis,[3,7] Maggie Kalev-Zylinska,[8] Yair Argon,[9] Shaun P. Jackson,[3,7] Philip Hogg,[2,3,†] and Freda H. Passam[1,4,†]

[1]Haematology Research Group, Heart Research Institute, Sydney, Australia; [2]The Centenary Institute, Sydney, Australia; [3]University of Sydney, Sydney, Australia; [4]Faculty Medicine Health, Central Clinical School, University of Sydney, Sydney, Australia; [5]Faculty Medicine Health, School of Medical Sciences, University of Sydney, Sydney, Australia; [6]Sydney Precision Bioinformatics Alliance, School of Mathematics and Statistics, University of Sydney, Sydney, Australia; [7]Thrombosis Research Group, Heart Research Institute, Sydney, Australia; [8]Department of Molecular Medicine and Pathology, School of Medical Sciences, University of Auckland, Auckland, New Zealand; and [9]Division of Cell Pathology, Children's Hospital of Philadelphia and University of Pennsylvania, Philadelphia, PA

**Key Points**

- ERp5 inhibits the activation of ER stress sensors protein kinase RNA-like endoplasmic reticulum kinase and IRE1 in murine platelets.
- In ERp5-deficient platelets, defective ER homeostasis promotes secretion of ER PDIs and chaperones.

Extracellular protein disulfide isomerases (PDIs), including PDI, endoplasmic reticulum protein 57 (ERp57), ERp72, ERp46, and ERp5, are required for in vivo thrombus formation in mice. Platelets secrete PDIs upon activation, which regulate platelet aggregation. However, platelets secrete only ~10% of their PDI content extracellularly. The intracellular role of PDIs in platelet function is unknown. Here, we aim to characterize the role of ERp5 (gene *Pdia6*) using platelet conditional knockout mice, platelet factor 4 (Pf4) $Cre^{+}$/$ERp5^{floxed\ (fl)/fl}$. $Pf4Cre^{+}$/$ERp5^{fl/fl}$ mice developed mild macrothrombocytopenia. Platelets deficient in ERp5 showed marked dysregulation of their ER, indicated by a twofold upregulation of ER proteins, including PDI, ERp57, ERp72, ERp46, 78 kilodalton glucose-regulated protein (GRP78), and calreticulin. ERp5-deficient platelets showed an enhanced ER stress response to ex vivo and in vivo ER stress inducers, with enhanced phosphorylation of eukaryotic translation initiation factor 2A and inositol-requiring enzyme 1 (IRE1). ERp5 deficiency was associated with increased secretion of PDIs, an enhanced response to thromboxane A2 receptor activation, and increased thrombus formation in vivo. Our results support that ERp5 acts as a negative regulator of ER stress responses in platelets and highlight the importance of a disulfide isomerase in platelet ER homeostasis. The results also indicate a previously unanticipated role of platelet ER stress in platelet secretion and thrombosis. This may have important implications for the therapeutic applications of ER stress inhibitors in thrombosis.



Submitted 29 June 2022; accepted 17 November 2022; prepublished online on *Blood Advances* First Edition 12 December 2022; final version published online 26 April 2023. https://doi.org/10.1182/bloodadvances.2022008457.

*A.J.L. and A.D. contributed equally to this study.

†P.H. and F.H.P. are joint senior authors.

The mass spectrometry proteomics data reported in this article have been deposited to the ProteomeXchange Consortium via the PRIDE partner repository (data set identifier PXD034094; username: reviewer_pxd034094@ebi.ac.uk and password: vQZZdlaJ).

Data are available on request from the corresponding author, Freda H. Passam (freda.passam@sydney.edu.au).

The full-text version of this article contains a data supplement.

## Introduction

Platelets promote thrombus formation upon activation by releasing α and dense granules. However, platelet releasates also contain nongranule proteins, such as the endoplasmic reticulum protein (ERp) protein disulfide isomerase (PDI),[1] which platelets externalize by nonconventional secretory pathways.[2] Multiple other members of the PDI family have been identified in the platelet releasate,[3] including ERp57,[4] ERp72,[5] ERp46,[6] and ERp5.[7] Using inhibitory antibodies or platelet conditional gene knockout (CKO) models, it was shown that released PDI, ERp57, ERp72, ERp46, and ERp5 promote platelet aggregation and thrombus formation.[8-11] However, the intracellular role of platelet PDIs has not been studied previously.

In nucleated cells, the primary role of PDIs is to catalyze protein folding in the ER.[12] PDIs are disulfide oxidoreductases that catalyze the oxidation and reduction of disulfide bonds to enable protein folding. The folding activity of PDIs is aided by ER chaperones, such as 78 kilodalton glucose-regulated protein (GRP78).[13] PDI function is important in cells with high synthetic and secretory activity, such as β-pancreatic cells.[14] In conditions of excess protein production or oxidative stress, the folding capacity of the ER is exceeded, resulting in ER stress.[15] ER stress activates the unfolded protein response, which involves the compensatory activation of inositol-requiring enzyme 1 (IRE1), protein kinase RNA-like endoplasmic reticulum kinase (PERK), and activating transcription factor 6 (ATF6) pathway to resolve ER stress.[16]

ER stress develops in megakaryocytes at the stage of proplatelet formation.[17] However, there is limited knowledge of the function of ER stress in platelets. The ER in platelets, also known as the dense tubular system, regulates $Ca^{2+}$ homeostasis and prostanoid synthesis.[18] Being anucleate cells, platelets have limited protein synthesis despite high concentrations of PDIs, that is, 1 human platelet expresses ~32 000 PDI molecules.[19] It is, therefore, intriguing to consider the ER function of platelet PDIs. The PDIs may either be passively transferred to platelets from megakaryocytes or may have autonomous functions within the platelet ER. We sought to understand the function of ERp5 in platelets based on its intracellular function in other cells. In fibroblasts, ERp5 has been shown to play a pivotal role in the ER stress response by the inhibition of the IRE1 and PERK pathway.[20,21] Here, we investigated if ERp5 modulates ER stress responses in platelets using the first-described platelet ERp5 CKO mouse.

In our studies of the phenotype of ERp5 CKO mice, we observed that these mice had mild macrothrombocytopenia. The knockout of ERp5 in mouse platelets disrupted ER homeostasis, accompanied by an increased abundance of multiple ER disulfide isomerases and chaperone proteins and enhanced activation of the ER stress pathways, IRE1 and PERK. ERp5-deficient platelets were hypersecretory of ER proteins and displayed increased thrombus formation. These results support a physiological function of intracellular ERp5 in safeguarding from ER stress and accompanying platelet secretion.

## Methods

Reagents, platelet isolation and immunofluorescence, measurement of reticulated platelets, platelet transmission electron microscopy (TEM), bone marrow and spleen immunohistochemistry, platelet proteomics, western blot of platelet lysates and releasates, disulfide reductase assay, enzyme-linked immunosorbent assay, platelet flow cytometry, aggregation, adhesion & clearance, tail bleeding time, activated partial thromboplastin time, and the carotid artery electrolytic method are presented in the supplemental Material.

### Generation of mice with CKO of ERp5 in megakaryocyte-platelet lineage

*Pdia6*$^{flox/flox}$ (ERp5$^{fl/fl}$) mice were produced by the Mouse Engineering at Garvan/ABR (MEGA) Facility (Moss Vale, Sydney, NSW, Australia) using CRISPR/Cas9 gene targeting in C57BL/6J mouse embryos following established molecular and animal husbandry techniques.[22] A single-guide RNA was employed that targeted Cas9 cleavage 79 base pairs (bp) 3′ of exon 2 of *Pdia6* (TGAGACAGGATCATTAG*CCGTGG; *, Cas9 cleavage site; underlined, protospacer-associated motif). A 3751 bp homologous recombination (HR) substrate was synthesized in pUC57 plasmid (Genscript, Piscataway, NJ), including 2500 bp 5′ and 760 bp 3′ homology arms either side of a loxP-flanked 423 bp insert containing exon 2 plus 202 bp and 79 bp of 5′ and 3′ flanking intron sequences, respectively. A solution consisting of the single-guide RNA (15 ng/μL), purified double-stranded HR substrate plasmid DNA (2 ng/μL), and full-length, polyadenylated *Streptococcus pyogenes* Cas9 messenger RNA (30 ng/μL) was prepared and microinjected into the nucleus and cytoplasm of C57BL/6J zygotes. Microinjected embryos were cultured overnight and those that underwent cleavage were introduced into pseudopregnant foster mothers. Pups were screened via polymerase chain reaction to detect the HR of the 2 loxP sites into 1 of the *Pdia6* alleles. Excision of exon 2 by Cre is predicted to create a frameshift after glycine-12 in ERp5, with translation terminating after the addition of 6 more residues. Mice were bred by crossing platelet factor 4 (Pf4) Cre$^{+}$/ERp5$^{fl/fl}$ with ERp5$^{fl/fl}$ mice to generate Pf4Cre$^{+}$ mice with ERp5-deficient platelets and Pf4Cre$^{-}$ littermate controls. All mice were genotyped using tail clips as a source of genomic DNA to detect the Pf4Cre and floxed *Pdia6* alleles. Protein expression was measured by western blot of washed platelet proteins separated by sodium dodecyl sulfate polyacrylamide gel electrophoresis. Sex and age-matched CKO (Pf4Cre$^{+}$/ERp5$^{fl/fl}$) and littermate controls (ERp5$^{fl/fl}$) were used in all experiments. All experiments were conducted in accordance with the approval from the University of Sydney Animal Ethics Committee (2017/1238).

### Induction of ER stress and $Ca^{2+}$ flux assay

Washed platelets were prepared at 400 × $10^3$/μL, volume 100 μL. Platelets were treated with 2 μM thapsigargin for 60 minutes, 2 μg/mL tunicamycin for 2 hours or equal volume of dimethyl sulfoxide (DMSO) buffer.[17,21,23] Separately, platelets were isolated from mice 24 hours after intraperitoneal injection of 1 μg/g tunicamycin or DMSO vehicle as the control.[24] Thapsigargin induces ER stress by inhibiting sarcoendoplasmic reticulum $Ca^{2+}$ ATPase, which leads to a rise in cytoplasmic $Ca^{2+}$ and depletion of the ER stores.[17] Tunicamycin induces ER stress by inhibiting N-linked glycosylation of proteins in the ER.[21,23]

Platelet lysates were separated by sodium dodecyl sulfate polyacrylamide gel electrophoresis using a 4% to 20% polyacrylamide gel. Primary antibodies to IRE1, phosphorylated (P)-IRE1, eukaryotic translation initiation factor 2A (eIF2a), P-eIF2a, c-Jun N-terminal kinase (JNK), P-JNK, spliced X-box binding protein 1 (XBP1), CCAAT-enhancer–binding protein homologous protein (CHOP),

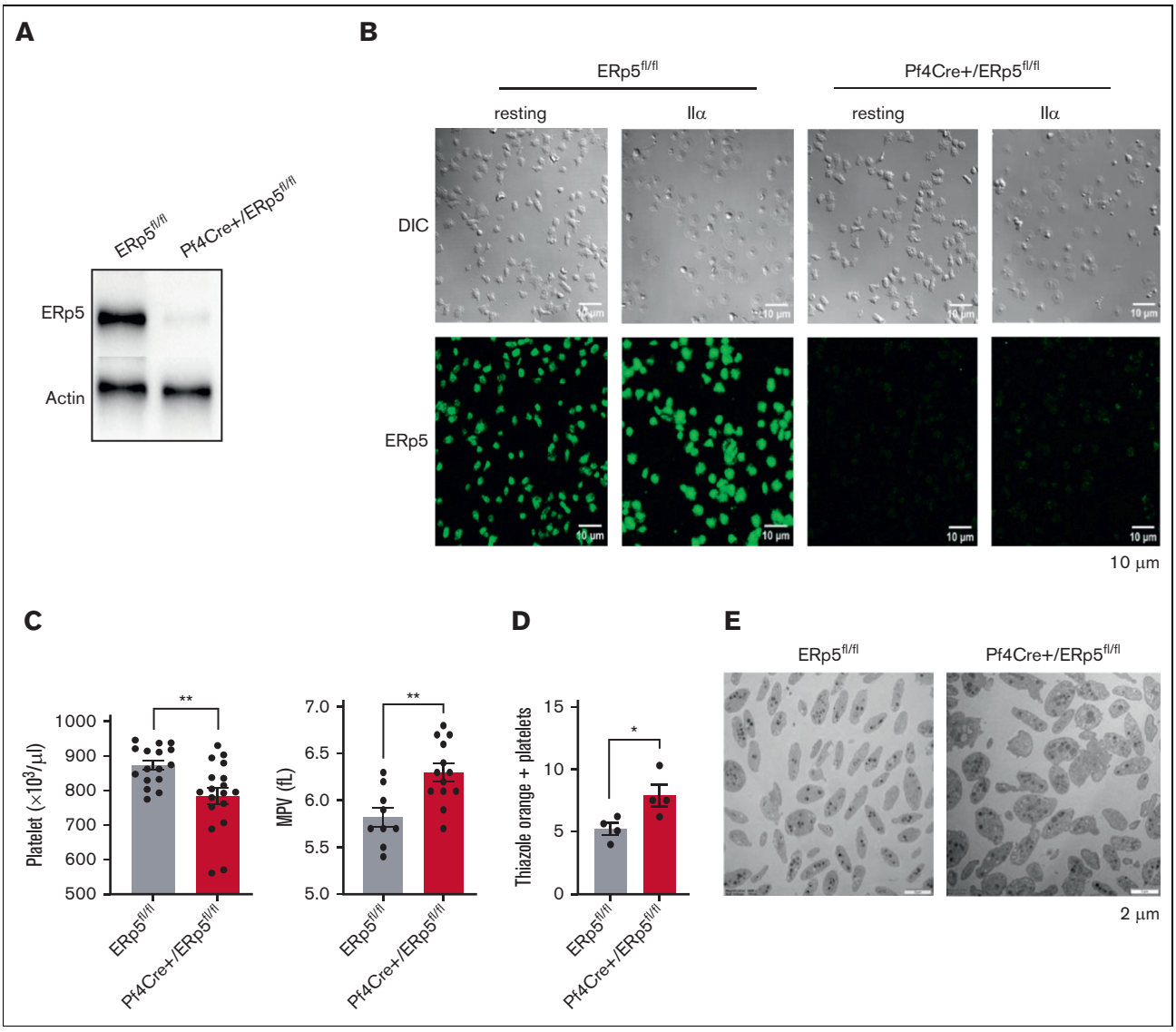


**Figure 1. Deletion of ERp5 in the megakaryocyte lineage results in mild macrothrombocytopenia.** (A) Western blot of ERp5 in resting platelet lysates from control ($ERp5^{fl/fl}$) and CKO ($Pf4Cre^{+}/ERp5^{fl/fl}$) mice, demonstrating ERp5 deletion in platelets. (B) Immunostaining of ERp5 in platelets from control and CKO mice after their adhesion to fibrinogen, without (resting) or with stimulation with thrombin (IIα). Differential interference contrast (DIC) (top) and staining with an anti-ERp5 Alexa 488 antibody (bottom). Representative images, n = 2 per genotype. (C) Peripheral platelet count and mean platelet volume (MPV) in control (gray column) and CKO mice (red column), n = 16 to 18 mice per genotype. (D) Percentage of reticulated (thiazole orange–positive) platelets in control and CKO mice. (E) Ultrastructure of resting platelets isolated from control and CKO mice. Representative TEM images showing increased platelet size in CKO mice. n = 4 mice per genotype for thiazole orange staining and TEM, mean ± standard error of the mean (SEM), Student *t* test. $^{*}P < .05$, $^{**}P < .005$. Scale bar, 10 μm (B) and 2 μm (E).

caspase 3, and ATF6 were probed at 1:1000 dilution with anti–β-actin or glyceraldehyde-3-phosphate dehydrogenase at 1:1000 dilution as loading control.

For intracellular $Ca^{2+}$ measurement, mouse platelets (200 × $10^3$/μL, volume 500 μL) were labeled with 15 μM Fura-2AM and Pluronic F-127 Plus N-2-hydroxyethylpiperazine-N′-2-ethanesulfonic acid–Tyrode buffer supplemented with 12.9 mM sodium citrate for 45 minutes at 37°C.[25] Platelets were recalcified with 1 mM $CaCl_2$ and 1 mM $MgCl_2$, allowed to rest for 3 minutes at 37°C, before stimulation with 0.2 μM U46619, 5 μM adenosine diphosphate (ADP), 0.1 U/mL thrombin, or 1 μg/mL collagen-related peptide (CRP). Relative $Ca^{2+}$ levels are reported as the ratio of the mean fluorescence emitted at 510 nm when excited alternatively at 340 and 380 nm (ratio, 340:380) using a CLARIOstar, BMG Labtech, Ortenberg, Germany.

## Carotid artery electrolytic injury–induced thrombosis

Mice were used between 16 and 20 weeks of age. The detailed method has recently been published.[26]

## Mesenteric vein laser injury–induced thrombosis

Matched mice were used between 8 and 10 weeks of age. Mice were intraperitoneally injected with 1 μg/g tunicamycin or DMSO vehicle, as described.[24] After 24 hours, mice were anesthetized, and

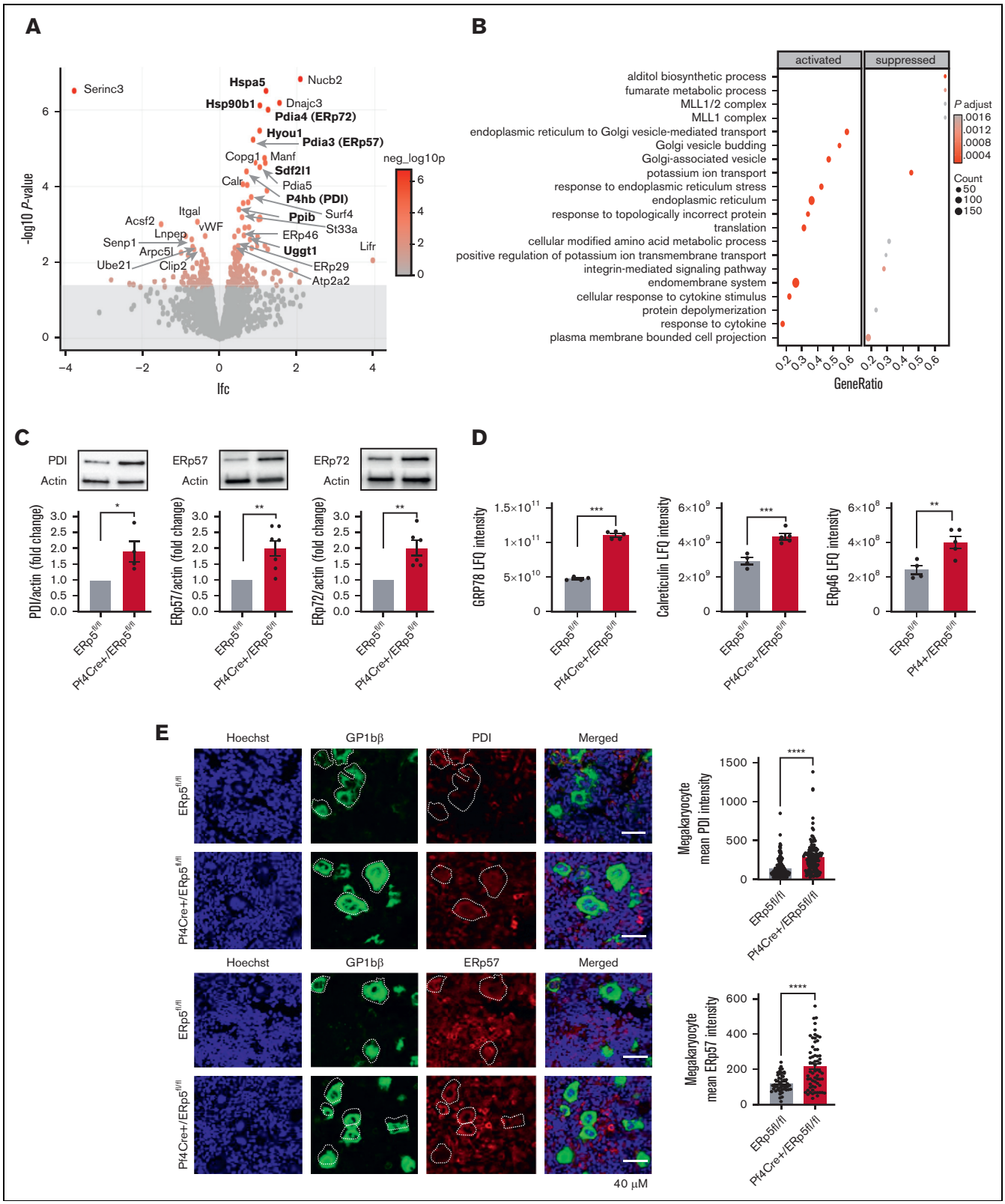


**Figure 2. Evidence of increased ER stress pathways in ERp5-deficient platelets.** (A) Proteomic analysis of resting platelet lysate from control (ERp5$^{fl/fl}$) and CKO (Pf4Cre$^{+}$/Erp5$^{fl/fl}$) mice. Volcano plot for all proteins detected by tandem mass spectometry (MS/MS), with the log2 fold change (lfc) plotted on the x-axis vs the negative log10 (*P*) of a paired test statistic on the y-axis. Proteins in red are significantly increased (positive lfc value) or decreased (negative lfc value) in CKO compared with control mice ($P < .05$). Color scale represents negative log10 (*P*); $P = .05$ corresponds to a negative log10 *P* value of 1.3 (upper limit of grayed-out area). (B) Upregulated and downregulated protein

**Table 1. Top 10 increased proteins in lysates of resting ERp5 knockout platelets**

| | Protein | Name | Log FC | Average expression | *P* | Adjusted *P* | Function | Intracellular location |
|---|---|---|---|---|---|---|---|---|
| 1 | Nucb2 | Nucleobindin-2 | 2.0 | 27.6 | 0 | .0002 | $Ca^{2+}$ binding | ER cytoplasm |
| 2 | Hspa5 | 78 kilodalton glucose-regulated protein | 1.2 | 34.8 | 0 | .0002 | ER chaperone | ER |
| 3 | Dnajc3 | DnaJ homolog subfamily C member 3 | 1.5 | 29.7 | 0 | .0004 | Unfolded protein response, inhibition of phosphorylation of eIF2a | ER |
| 4 | Hsp90b1 | Endoplasmin | 1.0 | 34.1 | 0 | .0004 | ER chaperone, transport of secreted proteins | ER |
| 5 | Pdia4 (ERp72) | Protein disulfide isomerase A4 | 1.2 | 31.4 | 0 | .0005 | Disulfide isomerase | ER |
| 6 | Hyou1 | Hypoxia upregulated protein 1 | 1.0 | 31.7 | 0 | .0013 | Hypoxia upregulated, ER stress | ER |
| 7 | Pdia3 (ERp57) | Protein disulfide isomerase A3 | 0.8 | 34.3 | 0 | .0016 | Disulfide isomerase | ER |
| 8 | Manf | Mesencephalic astrocyte–derived neurotrophic factor | 1.1 | 30.9 | 0 | .0057 | Hypoxia upregulated, ER stress | ER |
| 9 | Copg1 | Coatomer subunit gamma-1 | 0.9 | 28.4 | 0 | .0063 | Protein transport from the ER to Golgi vesicles | Cytoplasm |
| 10 | Sdf2l1 | Stromal cell-derived factor 2-like protein 1 | 1.2 | 29.2 | 0 | .0066 | Chaperone cofactor | ER |

Protein function data have been sourced from UniProt.
Log FC, log fold change.

the inferior vena cava was located and injected with 0.1 μg/g anti-mouse glycoprotein Ibβ (CD42c) Dylight 488. The mesentery was exteriorized and spread onto a coverslip. The mesenteric vein was located under the eyepiece, and the focal plane focused on the endothelial cell layer. The mesentery was perfused with warmed normal saline throughout the experiment. Laser injury to the endothelial cell layer was induced with the RAPP laser module from Rapp OptoElectronic GmbH, Hamburg, Germany. Laser power was set at 10% and pulsed 5 times, 300 ms each pulse, in a 10 $\mu m^2$ sized square. The laser injury was performed on 3 to 4 veins per mouse. The area of the platelet fluorescence at 12 μm above the base of the veins was measured over time in accordance with what has recently been described.[27] Analysis was performed using image J.

### Statistical analysis

Normal distribution of data was confirmed by the Shapiro-Wilk test. Comparison of 2 groups was performed by Student *t* test. Comparison of multiple groups was performed by 1-way analysis of variance with Dunn post hoc test. $P \leq .05$ were considered as statistically significant. Analysis was performed using the GraphPad Prism 8.0 software.

For all proteomics data, statistical analysis employed the limma R package.[28] Gene ontology enrichment pathways were identified with clusterprofiler R package.[29] Details are provided in the supplemental Material.

## Results

### Deletion of ERp5 in the megakaryocyte lineage results in decreased platelet count and larger platelets

Polymerase chain reaction analysis of genomic DNA confirmed homologous integration of *Pdia6*-floxed alleles carrying Pf4 Cre recombinase. Expression of the ERp5 protein, tested by western blotting of platelet lysates and immunofluorescent staining of adherent platelets, confirmed the effective deletion of ERp5 in the platelets of $Pf4Cre^{+}/ERp5^{fl/fl}$ mice (Figure 1A-B).

Measurement of the full blood count showed that the white blood cell count, red blood cell count, and hemoglobin were not statistically different between $Pf4Cre^{+}/ERp5^{fl/fl}$ and $ERp5^{fl/fl}$ mice (supplemental Table 1). However, the platelet count was significantly decreased in $Pf4Cre^{+}/ERp5^{fl/fl}$ mice compared with that in $ERp5^{fl/fl}$ mice (Figure 1C). Platelets of $Pf4Cre^{+}/ERp5^{fl/fl}$ mice were also larger than those of $ERp5^{fl/fl}$ ones, with significantly increased mean platelet volume (Figure 1C; supplemental Table 1). Reticulated platelets increased in $Pf4Cre^{+}/ERp5^{fl/fl}$ mice compared with those in $ERp5^{fl/fl}$ mice, as measured by thiazole orange positivity (Figure 1D) of gated platelets with the same size (supplemental Figure 1).[30] The increased size of ERp5-deficient platelets was confirmed by TEM (Figure 1E), whereas cytoskeletal staining (supplemental Figure 2A) and α and dense granule density per $\mu m^2$

**Figure 2 (continued)** pathways in the resting platelet lysate of CKO mice by gene ontology enrichment pathway analysis. (C) Western blot of resting platelet lysates from control (gray) and CKO (red) mice showing increased expression of PDI, ERp57, and ERp72 proteins in ERp5-deficient platelets. Top panels are representative blots. Bottom panels show the relative band density of protein, expressed as a ratio to the corresponding β-actin band, n = 4 to 7 per genotype. (D) Label-free quantification (LFQ) intensity plots for ER proteins GRP78, calreticulin, and ERp46 detected by MS/MS in the resting platelet lysates from control (gray) and CKO (red) mice, n = 4 to 5 per genotype. (E) Megakaryocyte expression of PDI and ERp57 in the bone marrow of control and CKO mice. Representative bone marrow histology sections, stained for Hoechst (nuclei, blue), GP1bβ (green), PDI, or ERp57 (red). Mean fluorescence intensity per megakaryocyte area. n = 28 to 35 megakaryocytes from 3 to 4 mice per genotype, mean ± SEM, Student *t* test. $^{*}P < .05$, $^{**}P < .005$, $^{***}P < .0005$, $^{****}P < .0001$.

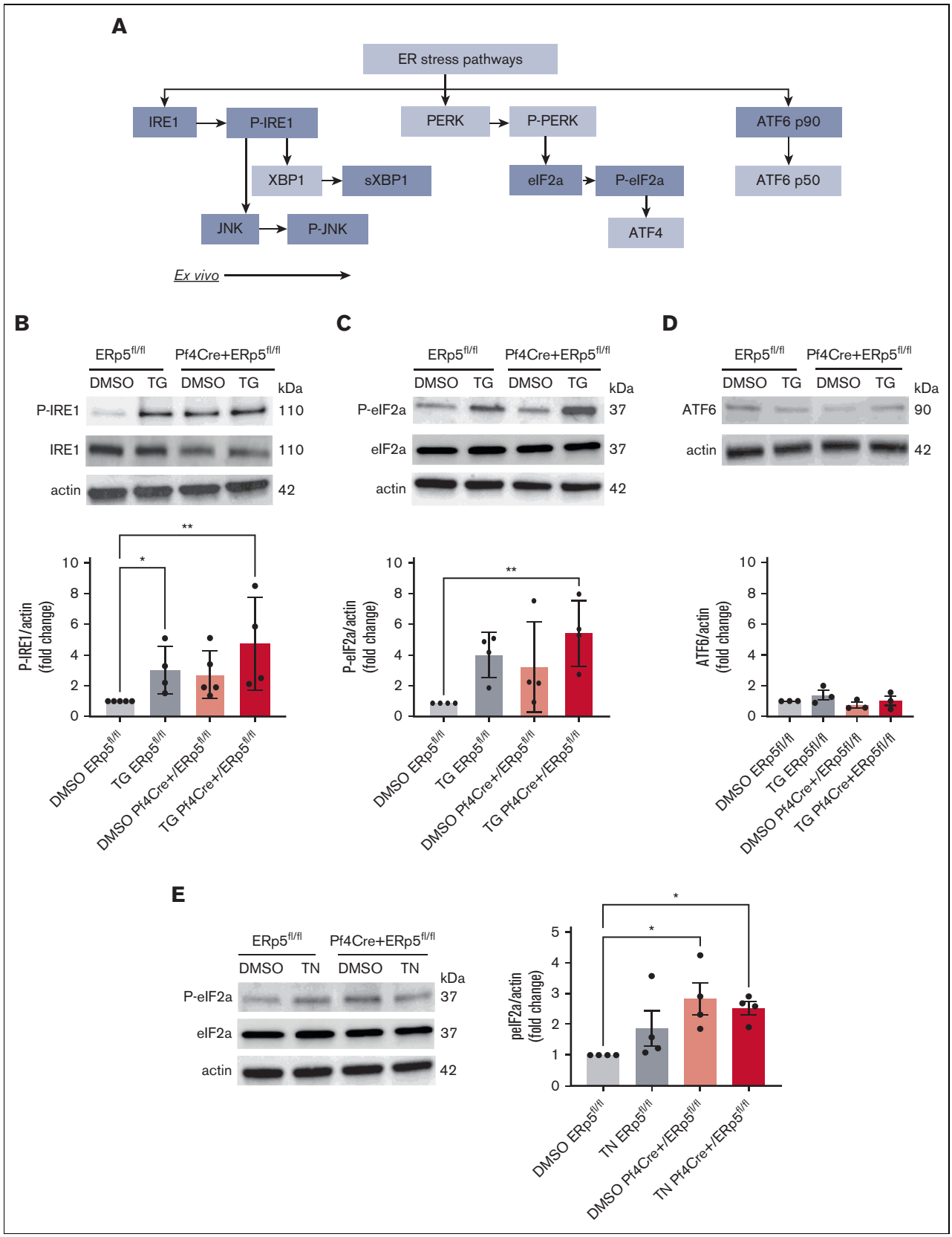


**Figure 3. ERp5-deficient platelets have increased activation of the PERK pathway.** (A) Schematic of the 3 ER stress/unfolded protein response pathways: IRE1, PERK, and ATF6. Proteins included in this study are highlighted in gray. Detection of P-IRE1, IRE1 (B); P-eIF2a, eIF2a (C); and ATF6 (D) in platelet lysates from control (ERp5$^{fl/fl}$) and CKO (Pf4Cre$^{+}$/ERp5$^{fl/fl}$) mice after treatment of platelets with DMSO (vehicle control) or thapsigargin (TG). Representative immunoblots are shown. Band densitometry of P-IRE1, P-eIF2a, and ATF6

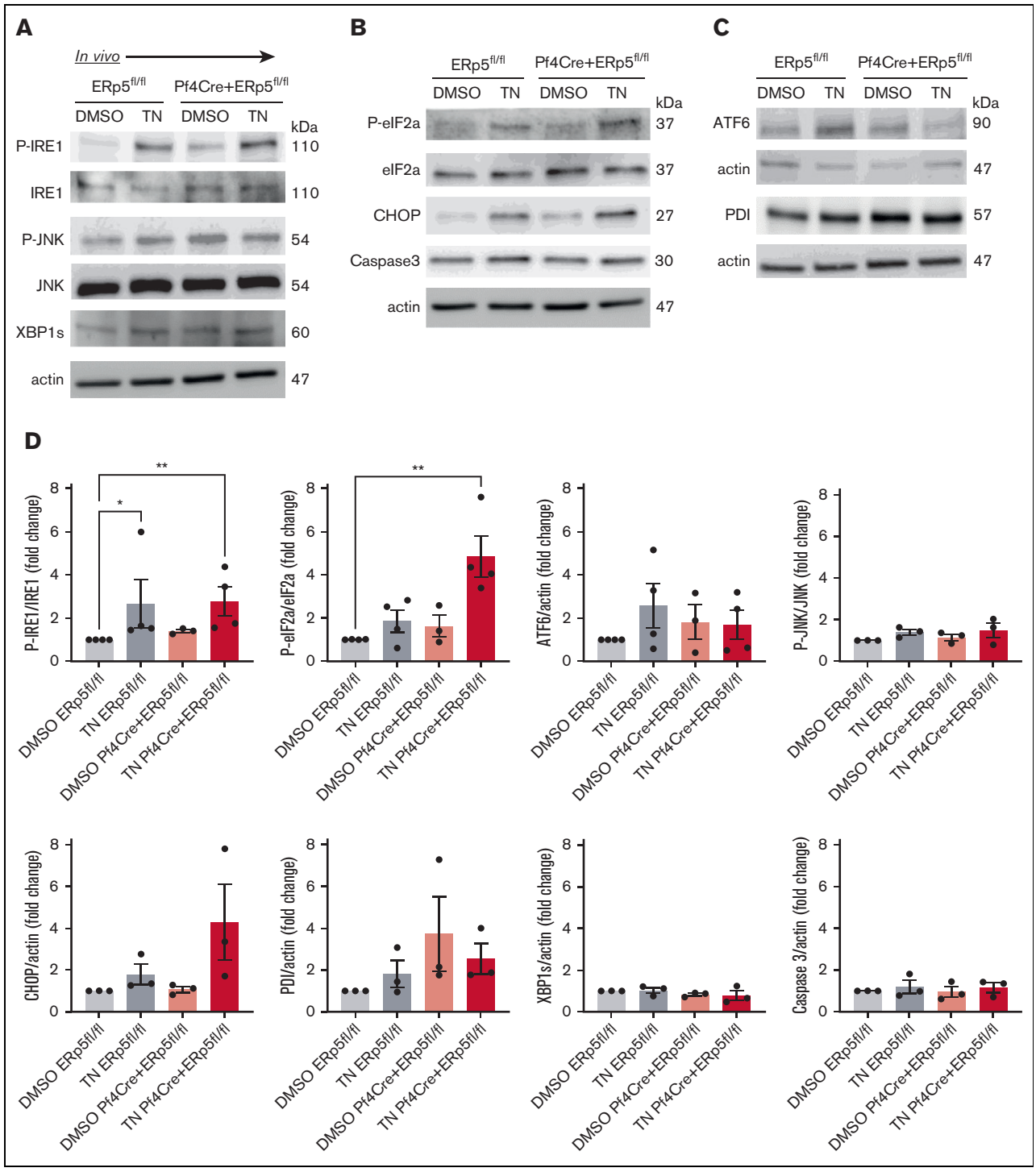


**Figure 4. Injection of tunicamycin induces platelet ER stress in ERp5 CKO mice.** Detection of P-IRE1, IRE1, P-JNK, JNK, and XBP1s (A); (B) P-eIF2a, eIF2a, CHOP, and caspase 3 (B); and ATF6 and PDI (C) in platelets isolated from control (ERp5$^{fl/fl}$) and CKO (Pf4Cre$^{+}$/ERp5$^{fl/fl}$) mice 24 hours after injection with DMSO (control) or tunicamycin (TN). Representative immunoblots are shown. Band densitometry of P-IRE1; P-JNK expressed as a ratio to total protein. XBP1s is expressed as a ratio to actin. P-eIF2a is expressed as a ratio to total eIF2a. CHOP, caspase 3, ATF6, and PDI are expressed as ratios to actin in control (gray) and KO (red) platelets after injection of DMSO (light box) and TN (dark box). Ratios are presented as fold change over DMSO-treated controls. n = 3 to 4 mice per genotype, mean ± SEM, 1-way ANOVA with Dunn post hoc analysis. $^{**}P < .005$, $^{*}P < .05$.

**Figure 3 (continued)** expressed as a ratio to corresponding β-actin bands, in control (gray) and KO (red) platelets after treatment with DMSO (light box) or TG (dark box). (E) Detection of P-eIF2a and eIF2a in platelets after treatment with DMSO or tunicamycin (TN) for 2 hours. Representative immunoblots are shown. Band densitometry of P-eIF2a expressed as a ratio to corresponding β-actin bands, in control (gray) and KO (red) platelets after treatment with DMSO (light box) or TN (dark box). Ratios are presented as fold change over DMSO-treated controls. n = 3 to 4 mice per genotype, mean ± SEM, 1-way analysis of variance (ANOVA) with Dunn post hoc analysis. $^{*}P < .05$, $^{**}P < .005$. kDa, kilodalton.

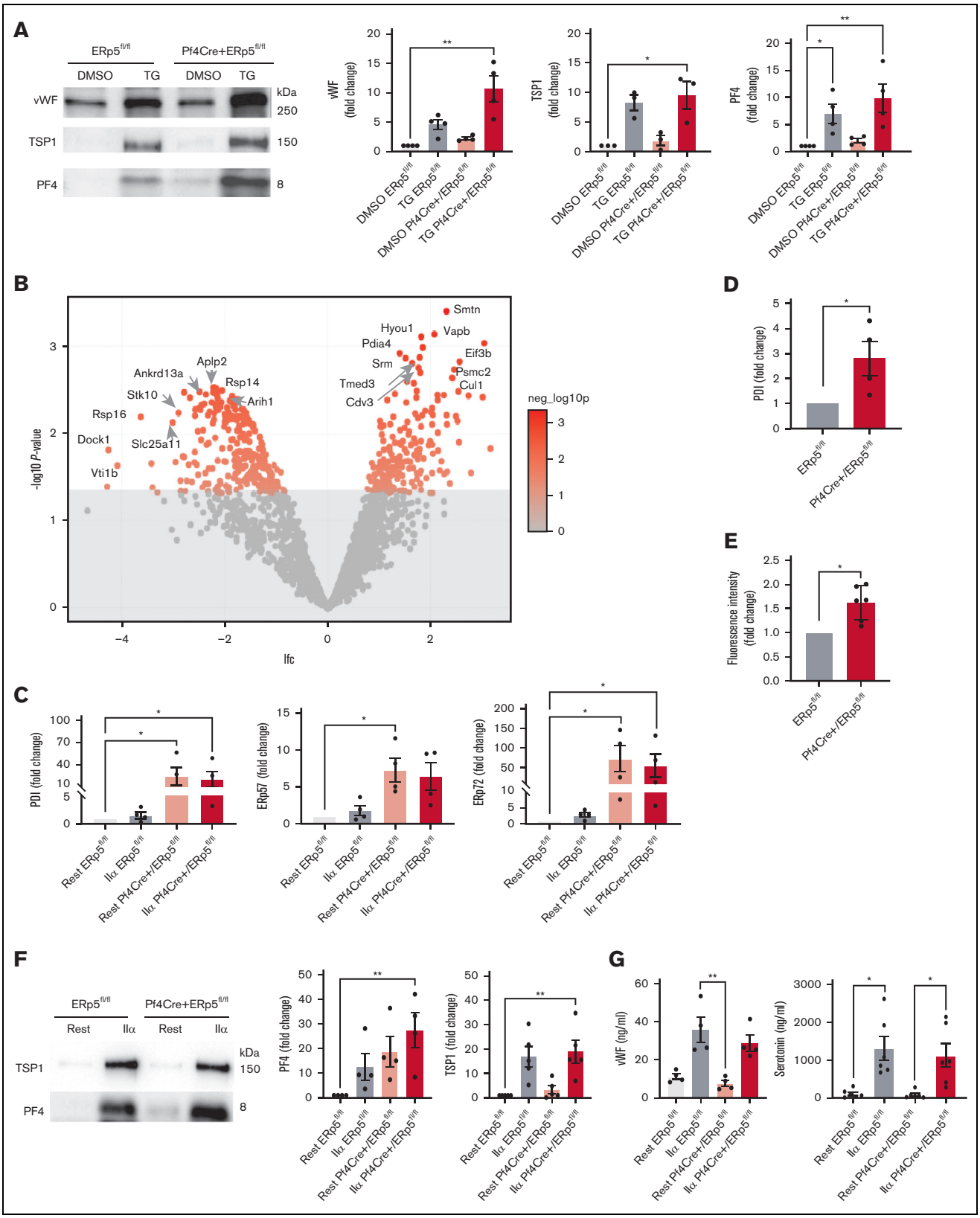


**Figure 5. ERp5-deficient platelets have increased constitutive secretion of ER proteins.** (A) Representative immunoblots of vWF, TSP1, and PF4 in the platelet releasates from control (ERp5$^{fl/fl}$) and CKO (Pf4Cre$^{+}$/ERp5$^{fl/fl}$) mice after treatment of platelets with DMSO (buffer control) or thapsigargin (TG). Densitometry of VWF, TSP1, and PF4 in the releasates from control (gray) or KO (red) platelets treated with DMSO (light box) or TG (dark box). Ratios are presented as fold change over DMSO-treated controls. (B) Proteomic analysis of resting platelet releasate from ERp5$^{fl/fl}$ and Pf4Cre$^{+}$/ERp5$^{fl/fl}$ mice. Volcano plot for all proteins detected by MS/MS, with the log2 fold change (lfc)

**Table 2. Top 10 increased platelet proteins in releasate of resting ERp5 knockout platelets**

| | Protein | Name | Log FC | Average expression | *P* | Adjusted *P* | Function | Intracellular location |
|---|---|---|---|---|---|---|---|---|
| 1 | Smtn | Smoothelin | 2.3 | 25.9 | .0004 | .1376 | Structural protein, stress fibers | Cytoskeleton |
| 2 | Vapb | Vesicle-associated membrane protein–associated protein B | 2.0 | 26.1 | .0007 | .1376 | Vesicle trafficking | Vesicular membranes, cytoplasm |
| 3 | Hyou1 | Hypoxia upregulated protein 1 | 1.8 | 30.2 | .0008 | .1376 | Hypoxia upregulated, ER stress | ER |
| 4 | Eif3b | Eukaryotic translation initiation factor 3 subunit B | 3.0 | 26.7 | .0009 | .1376 | Initiation of messenger RNA translation | Cytoplasm |
| 5 | Psmc2 | 26S protease regulatory subunit 7 | 1.8 | 27.0 | .001 | .1376 | Adenosine triphosphate–dependent degradation of ubiquitinated proteins | cytoplasm |
| 6 | Pdia4 (ERp72) | Protein disulfide isomerase A4 | 1.4 | 31.3 | .0012 | .1376 | Disulfide isomerase | ER |
| 7 | Tmed3 | Transmembrane emp24 domain-containing protein 3 | 1.7 | 26.1 | .0013 | .1376 | Vesicular protein trafficking | ER, Golgi |
| 8 | Srm | Spermidine synthase | 1.5 | 27.5 | .0014 | .1376 | Polyamine biosynthesis | Cytoplasm |
| 9 | Cul1 | Cullin-1 | 2.5 | 23.6 | .0015 | .1376 | Protein ubiquitination | Cytoplasm |
| 10 | Cdv3 | Protein Cdv3 | 1.6 | 26.5 | .0016 | .1376 | Unknown, related to platelet activation[37] | Cytoplasm |

Protein function data have been sourced from UniProt and PubMed.
Log FC, log fold change.

on TEM were similar between Pf4Cre$^{+}$/ERp5$^{fl/fl}$ and ERp5$^{fl/fl}$ mice (supplemental Figure 2B). The expression of platelet surface receptors: integrin αIIb (CD41), CD42c, and glycoprotein VI was not different between Pf4Cre$^{+}$/ERp5$^{fl/fl}$ and ERp5$^{fl/fl}$ platelets (supplemental Figure 2C). In addition, Pf4Cre$^{+}$/ERp5$^{fl/fl}$ and ERp5$^{fl/fl}$ platelets were not different in the expression of surface P-selectin and activated αIIbβ3 integrin (JON/A) in response to increasing doses of thrombin (0.025-0.5 U/mL) (supplemental Figure 2D). Pf4Cre$^{+}$/ERp5$^{fl/fl}$ and ERp5$^{fl/fl}$ mice had similar tail bleeding times and activated partial thromboplastin time (supplemental Table 1; supplemental Figure 3A-C). The decreased platelet count in Pf4Cre$^{+}$/ERp5$^{fl/fl}$ mice was attributed to decreased platelet production, and not increased platelet removal, as platelet clearance was similar in Pf4Cre$^{+}$/ERp5$^{fl/fl}$ and ERp5$^{fl/fl}$ mice (supplemental Figure 3D).

Bone marrow and spleen megakaryocytes from Pf4Cre$^{+}$/ERp5$^{fl/fl}$ and ERp5$^{fl/fl}$ mice showed comparable counts and surface areas (supplemental Figure 4A-B). Pf4Cre$^{+}$/ERp5$^{fl/fl}$ megakaryocytes showed a significant increase in emperipolesis, with >30% of megakaryocytes containing neutrophils (supplemental Figure 4C).

## ERp5-deficient platelets have dysregulated ER

Proteomic analysis of resting platelets, isolated from Pf4Cre$^{+}$/ERp5$^{fl/fl}$ and ERp5$^{fl/fl}$ mice, showed that ERp5 deficiency was associated with a striking increase in intracellular ER chaperones GRP78 (Hspa5), DnaJ homolog subfamily C member 3 (Dnajc3), endoplasmin (Hsp90b1), disulfide isomerases ERp72 and ERp57 (Figure 2A), and enriched ER stress and Golgi transport pathways (Figure 2B). The top 10 increased proteins are shown in Table 1. ERp5-deficient platelet lysates had an approximately twofold increase in PDI, ERp57, and ERp72 using western blot (Figure 2C) and a twofold increase in GRP78, calreticulin, and ERp46 using mass spectrometry compared with ERp5-replete platelet lysates (Figure 2D). A twofold increase in expression of PDI and ERp57 was also found in megakaryocytes of Pf4Cre$^{+}$/ERp5$^{fl/fl}$ mice compared with ERp5$^{fl/fl}$ mice (Figure 2E). In human hepatoma and mouse lymphoma cells, ERp5 is part of a large chaperone multiprotein complex including DnaJ homolog subfamily B member 11 (Dnajb11), Hsp90b1, GRP78, hypoxia upregulated protein 1 (Hyou1), stromal cell-derived factor 2-like protein 1 (Sdf2l1), ERp72 (Pdia4), PDI, and ERp29.[31] All of these complex members were significantly increased in ERp5-deficient platelets (Figure 2A). Proapoptotic proteins, including caspase 3, BAX, and Bcl-2 homologous antagonist/killer (Bak1),[32] were not significantly elevated in resting ERp5-deficient platelets compared with controls (supplemental Figure 5A).

## ERp5-deficient platelets have enhanced ER stress response to ex vivo treatment with thapsigargin and tunicamycin

Disulfide isomerases are increased during ER stress in cardiovascular[33] and neurodegenerative disease.[34] Thus, we questioned

**Figure 5 (continued)** plotted on the x-axis vs the negative log10 (*P*) of a paired test statistic on the y-axis. Proteins in red are significantly increased (positive lfc value) or decreased (negative lfc value) in CKO compared with control mice ($P < .05$). Color scale represents negative log10 (*P*), $P = .05$ corresponds to a negative log10 (*P*) of 1.3 (upper limit of grayed-out area). (C) Densitometry of PDI, ERp57, and ERp72 on western blots of platelet releasates from control (gray) and ERp5 CKO (red) mice after platelet treatment with buffer (rest) (light box) or thrombin 0.5 U/mL (IIα) (dark box). (D) CKO mice have increased plasma PDI. Densitometry of PDI on a western blot of plasma samples from control (gray) and CKO (red) mice. (E) Relative disulfide reductase activity of thrombin 0.5 U/mL-treated CKO platelets (red) compared with thrombin-treated control platelets (gray) as measured by the dieosin glutathione disulfide assay. (F) Representative immunoblots of TSP1 and PF4 in the platelet releasate after treatment with buffer (rest) or thrombin (IIα). Densitometry of TSP1 and PF4 in the releasates of control (gray) and ERp5 KO (red) platelets treated with buffer (light box) or thrombin (dark box). Ratios are presented as fold change over buffer-treated controls. (G) VWF and serotonin concentration (ng/mL) measured by enzyme-linked immunosorbent assay in the releasates of control (gray) and ERp5 KO (red) platelets treated with buffer (light box) or thrombin (dark box). n = 3 to 6 per genotype, mean ± SEM, Student *t* test (D, E), 1-way ANOVA with Dunn post hoc analysis (A, C, F, G). $^{*}P < .05$, $^{**}P < .005$.

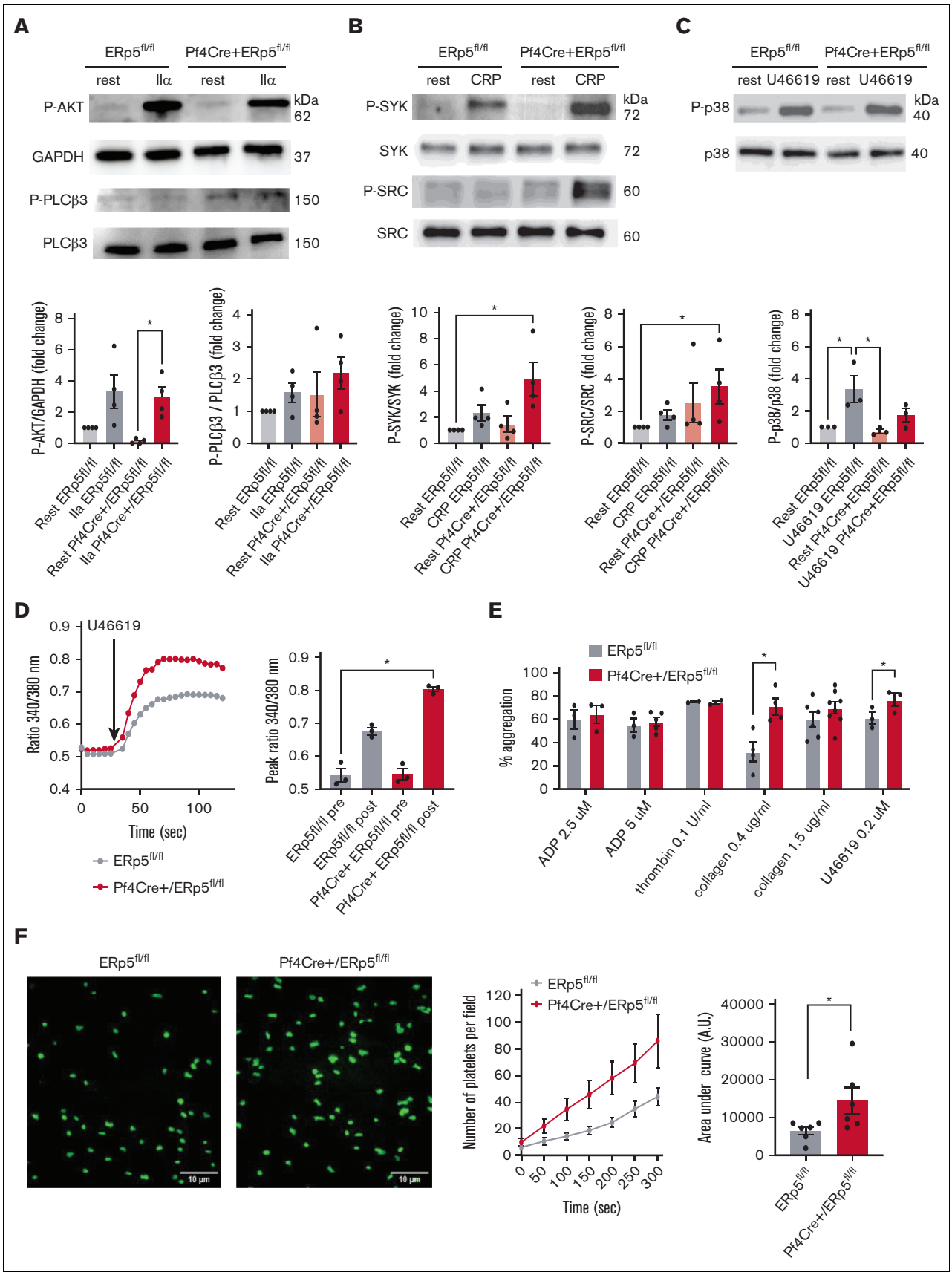


**Figure 6.**

whether ER stress was present in ERp5-deficient platelets. We measured the protein expression of members of the 3 ER stress pathways: IRE1, PERK, and ATF6 (Figure 3A). Compared with DMSO vehicle-treated ERp5$^{fl/fl}$ platelets, thapsigargin-treated Pf4Cre$^{+}$/ERp5$^{fl/fl}$ and ERp5$^{fl/fl}$ platelets showed increased P-IRE1 (Figure 3B), whereas only thapsigargin-treated Pf4Cre$^{+}$/ERp5$^{fl/fl}$ platelets showed increased P-eIF2a (downstream of PERK) (Figure 3C). Neither Pf4Cre$^{+}$/ERp5$^{fl/fl}$ nor ERp5$^{fl/fl}$ thapsigargin-treated platelets increased ATF6 (Figure 3D). Increased P-eIF2a was also observed in platelets from Pf4Cre$^{+}$/ERp5$^{fl/fl}$ mice, both at baseline and after treatment with tunicamycin (Figure 3E). There was no difference in the baseline expression of CHOP, which is activated downstream of both PERK and IRE1 (supplemental Figure 5B).

## ERp5-deficient platelets have enhanced ER stress response to in vivo treatment with tunicamycin

To understand whether ER stress in ERp5 deficiency is relevant in vivo, we injected Pf4Cre$^{+}$/ERp5$^{fl/fl}$ and ERp5$^{fl/fl}$ mice with tunicamycin 1 μg/g or DMSO, and platelets were isolated 24 hours later. Platelets from both Pf4Cre$^{+}$/ERp5$^{fl/fl}$ and ERp5$^{fl/fl}$ mice showed increased expression of P-IRE1 (Figure 4A) after tunicamycin injection, whereas only Pf4Cre$^{+}$/ERp5$^{fl/fl}$ platelets showed increased P-eIF2a (Figure 4B). There was no difference in ATF6 expression after tunicamycin injection (Figure 4C). ERp5-deficient platelets showed an increasing trend in CHOP expression after tunicamycin injection, which did not reach significance (Figure 4D). The expression of P-JNK, XBP1s, caspase 3, or PDI was not different between Pf4Cre$^{+}$/ERp5$^{fl/fl}$ and ERp5$^{fl/fl}$ mice (Figure 4D).

## ERp5-deficient platelets have increased constitutive secretion of ER proteins

Because thapsigargin-induced ER stress has previously been shown to increase platelet secretion,[35] we investigated if thapsigargin treatment enhanced the secretion in ERp5-deficient platelets. Platelets from Pf4Cre$^{+}$/ERp5$^{fl/fl}$ and ERp5$^{fl/fl}$ mice had no significant differences in the secretion of α-granule proteins, von Willebrand factor (vWF), thrombospondin 1 (TSP1), and PF4, at baseline or after treatment with thapsigargin (Figure 5A).

We then considered whether ER stress from ERp5 deficiency was associated with the secretion of other platelet proteins. Proteomic analysis of nonactivated platelet supernatants (releasates) identified an increase in proteins involved in protein synthesis and trafficking (Table 2). However, some proteins involved in protein processing (40S ribosomal protein S14 and ankyrin repeat domain-containing protein 13A) had decreased in the releasate and lysate of ERp5-deficient platelets (Figure 5B; supplemental Tables 2 and 3). Surprisingly, PDI, ERp57, and ERp72 had increased in the releasate of nonactivated ERp5-deficient platelets, whereas PDI and ERp72 also increased in the releasate of activated ERp5-deficient platelets compared with that of resting control platelets (Figure 5C). This was accompanied by increased plasma levels of PDI in Pf4Cre$^{+}$/ERp5$^{fl/fl}$ mice (Figure 5D). ERp5-deficient platelets showed enhanced reduction of the disulfide-containing fluorescent probe dieosin glutathione disulfide,[36] which is reduced by the PDIs and also by thioredoxin and glutaredoxin (Figure 5E). Platelets from Pf4Cre$^{+}$/ERp5$^{fl/fl}$ and ERp5$^{fl/fl}$ mice had no significant differences in the secretion of TSP1 and PF4 (Figure 5F) or vWF and dense granule serotonin (Figure 5G), at baseline or after stimulation with thrombin.

## ERp5-deficient platelets have increased signaling response to collagen and increased $Ca^{2+}$ flux and aggregation in response to thromboxane A2 ($TXA_2$) receptor agonist

Because ER stress and platelet signaling responses are dependent on $Ca^{2+}$ mobilization to the cytoplasm,[38] we investigated if ERp5 deficiency is accompanied by altered signaling pathways in platelets. Platelets from Pf4Cre$^{+}$/ERp5$^{fl/fl}$ and ERp5$^{fl/fl}$ mice were stimulated with thrombin, CRP, and U46619 ($TXA_2$ receptor agonist), followed by the detection of signaling proteins in the platelet lysate by western blot. Platelets from Pf4Cre$^{+}$/ERp5$^{fl/fl}$ and ERp5$^{fl/fl}$ mice had similar response to thrombin stimulation as assessed by the expression of P-AKT and P-phospholipase C (PLCβ3) (Figure 6A). Platelets from Pf4Cre$^{+}$/ERp5$^{fl/fl}$ mice showed increased phosphorylation of spleen tyrosine kinase (SYK) and proto-oncogene tyrosine-protein kinase Src (SRC) in response to CRP (Figure 6B). Platelets from Pf4Cre$^{+}$/ERp5$^{fl/fl}$ and ERp5$^{fl/fl}$ mice had similar expression of P-p38 in response to U46619 (Figure 6C). However, platelets from Pf4Cre$^{+}$/ERp5$^{fl/fl}$ mice stimulated with U46619 showed increased $Ca^{2+}$ flux with an elevated peak fluorescence ratio of 340:380 compared with ERp5$^{fl/fl}$ mice (Figure 6D). The $Ca^{2+}$ flux to 0.1 U/mL thrombin, 5 μM ADP, and 1 μg/mL CRP was not different between Pf4Cre$^{+}$/ERp5$^{fl/fl}$ and ERp5$^{fl/fl}$ mice (data not shown). A limitation of the $Ca^{2+}$ flux studies is that they studied the flux of extracellular $Ca^{2+}$ stores but not from intracellular stores.

Platelet aggregation was increased in platelets from Pf4Cre$^{+}$/ERp5$^{fl/fl}$ mice compared with ERp5$^{fl/fl}$ mice in response to low-

**Figure 6. ERp5-deficient platelets have enhanced activation of collagen signaling pathways, increased $Ca^{2+}$ mobilization and aggregation in response to U44619, and increased adhesion to fibrinogen under shear.** (A) Representative immunoblots of P-AKT and P-PLCβ3 in response to IIα stimulation. Band densitometry of P-AKT expressed as a ratio to glyceraldehyde-3-phosphate dehydrogenase (GAPDH); P-PLCβ3 expressed as a ratio to total protein in lysates of control ERp5$^{fl/fl}$ (gray) and CKO Pf4Cre$^{+}$/ERp5$^{fl/fl}$ (red) platelets treated with buffer (light box) or IIα (dark box). (B) Representative immunoblots of P-SYK and P-SRC in response to CRP stimulation. Band densitometry of P-SYK and P-SRC expressed as a ratio to the total protein in lysates of control (gray) and ERp5 KO (red) platelets treated with buffer (light box) or CRP (dark box). (C) Representative immunoblots of P-p38 and p38 in response to stimulation with 0.2 μm U46619. Band densitometry of P-p38 expressed as a ratio to the total protein in lysates of control (gray) and ERp5 KO (red) platelets treated with buffer (light box) or U46619 (dark box). All ratios are presented as fold change over buffer-treated controls. (D) Calcium flux, representative image, and peak $Ca^{2+}$ flux after stimulation of platelets from control ERp5$^{fl/fl}$ (gray) or CKO Pf4Cre$^{+}$/ERp5$^{fl/fl}$ (red) mice with U46619. (E) Aggregation (%) after activation with ADP, thrombin, collagen, and U46619. (F) Representative images of platelets labeled with calcein after perfusion on fibrinogen-coated microfluidic channels at a shear rate of 500 $s^{-1}$ for 5 minutes. Kinetics of adhesion of washed platelets from control (gray) and CKO (red) mice. Area under the curve (AUC) of platelet surface fluorescence at the end of perfusion (300 seconds) for control (gray) and CKO (red) platelets. n = 3 to 4 per genotype for signaling proteins; n = 3 to 6 per genotype for $Ca^{2+}$ flux, aggregation, and adhesion; mean ± SEM, Student *t* test (F), 1-way ANOVA with Dunn post hoc analysis (A-E). *$P < .05$.

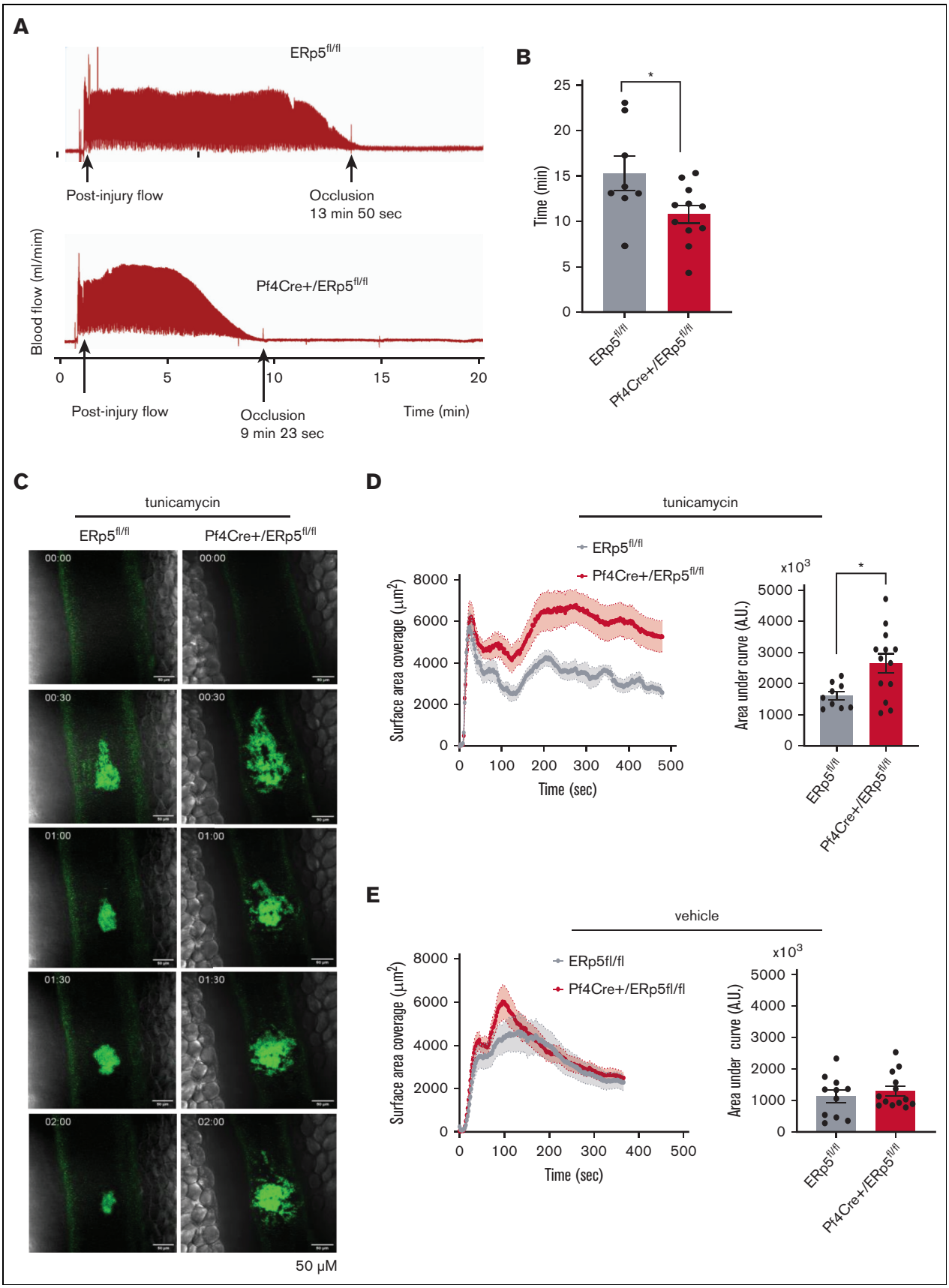


**Figure 7.**

dose U46619 and low-dose collagen, whereas platelet aggregation in response to ADP, thrombin, and higher doses of collagen was not different (Figure 6E). However, platelet aggregation of ERp5-deficient platelets in response to collagen was inhibited in the presence of 10 μM indomethacin ($TXA_2$ inhibitor),[7] suggesting that the heightened signaling and aggregation response of ERp5-deficient platelets to collagen is partially dependent on $TXA_2$ (supplemental Figure 6).

### ERp5-deficient platelets have increased platelet adhesion in vitro and thrombus formation in vivo

Because ERp5-deficient platelets have an increased secretion of PDI, ERp57, and ER72, we investigated if ERp5 deficiency affects platelet adhesion. Platelets from $Pf4Cre^{+}/ERp5^{fl/fl}$ mice showed increased adhesion to immobilized fibrinogen at a shear rate of 500 $s^{-1}$ compared with platelets from $ERp5^{fl/fl}$ mice (Figure 6F).

Next, we used an arterial model of in vivo thrombosis to measure the effect of platelet ERp5 deficiency on thrombus formation. The time to occlusion (zero flow) from thrombus formation was measured in carotid arteries subjected to electrolytic injury. $Pf4Cre^{+}/ERp5^{fl/fl}$ mice showed a shortened time to carotid occlusion compared with $ERp5^{fl/fl}$ mice (Figure 7A-B).

### Induction of ER stress potentiates thrombus formation of ERp5-deficient platelets in vivo

To investigate if ER stress plays a role in thrombus formation in vivo, we studied thrombus formation after intraperitoneal injection of tunicamycin 1 μg/g or DMSO vehicle as control. Both $Pf4Cre^{+}/ERp5^{fl/fl}$ and $ERp5^{fl/fl}$ mice appeared healthy 24 hours after injection of tunicamycin or DMSO. However, tunicamycin-injected $Pf4Cre^{+}/ERp5^{fl/fl}$ mice showed significantly increased platelet accumulation and thrombus size in response to laser-induced injury of the mesenteric veins as compared with tunicamycin-injected $ERp5^{fl/fl}$ mice (Figure 7C-D). Thrombus size was not significantly different between vehicle-injected $Pf4Cre^{+}/ERp5^{fl/fl}$ and $ERp5^{fl/fl}$ mice (Figure 7E).

## Discussion

This study reports a novel role for intracellular ERp5 in attenuating ER stress in platelets and safeguarding against hypersecretion of PDIs. Our analysis generated 3 key findings: (1) ERp5 plays a physiological role in ER homeostasis in the platelet/megakaryocyte lineage, (2) the absence of ERp5 upregulates other ER proteins and enhances ER stress responses in platelets, and (3) ERp5 deficiency leads to a prothrombotic tendency linked to enhanced secretion of PDIs and response to $TXA_2$.

ERp5 CKO mice developed mild macrothrombocytopenia, which has recently been identified in a human and mouse with ERp5 loss-of-function mutations.[39,40] Both mice and the index patient with mutant ERp5 developed diabetes and macrothrombocytopenia, suggesting a role for ERp5 in megakaryopoiesis. Previously, ERp57 has been shown to play a role in megakaryopoiesis by controlling intracellular $Ca^{2+}$. ERp57 acts as a "brake" for the activation of store-operated calcium entry (SOCE) by interacting with calreticulin and stromal interaction molecule 1 (STIM1).[41] The activation of SOCE and $Ca^{2+}$ mobilization activate signaling cascades that trigger proplatelet formation.[41] Whether ERp5 controls proplatelet formation via a similar mechanism is the subject of an ongoing study.

Deletion of platelet ERp5 increased the ER stress response primarily in the PERK pathway but not in the ATF6 pathway. Our findings are in agreement with previous studies where silencing of ERp5, in fibroblasts and β-pancreatic cells, enhanced the activation of IRE1 and PERK but not ATF6.[20,21] This enhancement was specific for ERp5, as silencing of PDI had no effect on IRE1 activation.[20] Silencing of ERp5 also induced the upregulation of ER proteins, including ERp72[21] and calreticulin, similar to what we observed in ERp5-deficient platelets. Other upregulated proteins are involved in vesicle transport (surfeit locus protein 4 [Surf4]), oligosaccharide transfer (dolichyl-diphosphooligosaccharide-protein glycosyltransferase subunit [STT3A]), and $Ca^{2+}$ transport (sarcoplasmic/endoplasmic reticulum calcium ATPase 2 [Atp2a2]) (supplemental File 3). In contrast, some of the downregulated platelet proteins are involved in protein processing and ubiquitinylation, such as leucyl-cystinyl aminopeptidase (Lnpep) and ubiquitin conjugating enzyme E2 I (Ube2i) (supplemental File 3), which may contribute to dysregulated ER function in ERp5 deficiency.

There is limited information on the results of dysregulated ER function in platelets. ER stress responses have been described in homocysteine-treated platelets from patients with diabetes.[23] Increased P-IRE1 has been recently reported in platelets from patients with diabetes and in tunicamycin-treated platelets, which is in line with our study.[42] Although ER stress has been shown to activate downstream apoptosis,[43,44] we did not find upregulation of apoptotic pathways in ERp5-deficient platelets. On the contrary, we found that ERp5 deficiency was associated with increased secretion of ER proteins. ER stress generally attenuates protein secretion from secretory cells (ie, β-pancreatic cells), but the secretion of ER chaperone proteins may increase. For example, ER stress in the heart, developing from decreased ER $Ca^{2+}$ in ischemia, stimulates the secretion of GRP78, GRP94, and calreticulin.[45] Secreted GRP78 stimulates prosurvival pathways in cultured cardiomyocytes.[45] In HEK293T cells, activation of the ATF6 pathway induces the secretion of the chaperone ERdj3. Secreted Erdj3 binds to misfolded proteins in the extracellular space, preventing protein aggregation.[46] In contrast, the increased release of PDIs from ERp5-deficient platelets may contribute to the prothrombotic tendency in ERp5 CKO mice.

**Figure 7. ERp5-deficient platelets have increased thrombotic tendency in vivo and enhanced thrombotic response after injection of tunicamycin.** (A-B) Doppler tracing of blood flow after electrolytic injury to the carotid artery in $ERp5^{fl/fl}$ (control) and $Pf4Cre^{+}/ERp5^{fl/fl}$ (CKO) mice (A) and time to occlusion after carotid electrolytic injury in control (gray) and CKO (red) mice (B); n = 6 to 11 per genotype. (C) Representative images of platelet (green) accumulation over time after laser injury of the mesenteric vein in a control and ERp5 CKO mouse injected with tunicamycin 24 hours prior. (D) Kinetics of mean ± SEM platelet accumulation over time as measured by fluorescence area and area under the curve (AU) of individual thrombi in control (gray) and CKO mice (red) after tunicamycin injection; n = 9 thrombi from 3 control mice and n = 13 thrombi from 4 CKO mice. (E) Kinetics of mean ± SEM platelet accumulation over time as measured by fluorescence area and AU of individual thrombi in control (gray) and CKO mice (red) after DMSO vehicle injection; n = 11 thrombi from 4 control mice and n = 13 thrombi from 4 ERp5 CKO mice, mean ± SEM, Student *t* test. $^{*}P < .05$.

Contributing to the prothrombotic tendency is the enhanced $TXA_2$ response of ERp5-deficient platelets. Although the mechanism is unknown, the prostaglandin pathway and $TXA_2$ generation primarily occurs in the ER,[18] so it is conceivable that ER stress locally may dysregulate key components of this pathway. Suppression of ER stress has been shown to decrease COX-1 expression and $TXA_2$ release from hypertensive rat aortas.[47] This raises the possibility that the signaling events and platelet aggregation seen in ERp5-deficient platelets are linked to dysregulated prostaglandin metabolism. Understanding the link between platelet ER stress and prostanoid synthesis is an important area for future investigation.

The effect of genetic deletion of platelet PDIs on signaling has not been studied to date.[6,11,19] However, the effect of disulfide isomerase genetic deletion on signaling in other cells is not without precedent. For example, using ERp57 knockout mouse embryonic fibroblasts, it was shown that the absence of ERp57 in the ER enhanced signal transducer and activator of transcription 3 (STAT3) activation.[48] The effect of PDIs on signaling may be different in the ER compared with the extracellular space. Exogenously added PDI is reported to inhibit $TXA_2$ receptor signaling via Ga13-mediated RhoA–guanosine triphosphate activation.[49] Although we identified an enhanced signaling response to CRP in ERp5-deficient platelets, this is likely secondary to $TXA_2$, as collagen-induced aggregation was inhibited by indomethacin.

The prothrombotic tendency of ERp5 CKO mice is context-dependent. There is not a global upregulation in platelet responsiveness to multiple agonists. Increased responsiveness to $TXA_2$ and hypersecretion of PDIs may be the major changes that are manifested under the experimental conditions described. This prothrombotic tendency contradicts previous findings, in which ERp5 function-blocking antibodies inhibited platelet aggregation[7] and thrombus formation.[10] However, these studies focused on the role of extracellular ERp5. The intracellular function of ERp5 could not have been probed by cell-impermeable antibodies and would require genetic deletion or cell-permeable inhibitors of ERp5. Using a genetic deletion approach, we identified an unexpected role of ERp5 in maintaining ER homeostasis in platelets. Genetic deletion of ERp5 caused upregulation and secretion of multiple ER proteins, including PDI, ERp57, and ERp72, which promote thrombus formation[8,9,11,50-53] and which, we presume, compensated for the lack of ERp5 in the extracellular compartment. The resulting mild prothrombotic phenotype, from ER dysregulation in ERp5 deficiency, was exacerbated after further ER challenge, that is, after the injection of tunicamycin.

Our finding of a cross talk between ER stress, secretion of PDIs, and prothrombotic tendency has interesting implications for pathological situations with increased ER stress, such as the metabolic syndrome and diabetes.[42] Patients with metabolic syndrome have increased platelet activity.[54] Our findings imply that increased ER stress could potentially contribute to platelet hyperactivity in the metabolic syndrome.[55]

In conclusion, we have identified ERp5 as an inhibitor of ER stress in platelets by attenuating the activity of PERK and IRE1. The most striking phenotype of ERp5-deficient platelets is platelet hypersecretion of ER proteins. ER stress inhibitors may play a role in cardiovascular medicine by decreasing platelet hyperactivity.

## Acknowledgments

The authors thank David Zahra and Robert Brink and the staff of MEGA, Garvan Institute, Sydney for the generation of the ERp5 conditional knockout mice; Ying Ying Su and Naveena Gokoolparsadh from the Australian Centre for Microscopy & Microanalysis, University of Sydney, for transmission electron microscopy imaging; and SydneyMS for providing the mass spectrometry instruments used in this study.

This research was funded by a Ramaciotti Foundations Health Investment Grant (F.H.P.), an NSW Health Cardiovascular Early Mid Researcher Grant (F.H.P.), and the National Health and Medical Research Council of Australia (grant 1143400) (P.H. and F.H.P.).

## Authorship

Contribution: F.H.P. and P.H. conceived the study, supervised research, designed experiments, and cowrote the manuscript; A.J.L. and A.D. designed and performed experiments, analyzed data, and cowrote the manuscript; L.H., J.T., Y.K., J.C., Z.Q., D.S., E.G., and M.E. performed experiments and analyzed data; J.M. and B.H. performed the carotid electrolytic injury model; M.L. performed and analyzed mass spectrometry data; Y.Z. and J.Y. performed the statistical analysis and presentation of mass spectrometry data; and S.P.J., M.K.-Z., and Y.A. cowrote the manuscript.

Conflict-of-interest disclosure: The authors declare no competing financial interests.

ORCID profiles: M.L., 0000-0002-8579-2267; Y.Z., 0000-0003-2173-3185; J.Y., 0000-0002-5271-2603; J.C., 0000-0001-8910-8664; Z.Q., 0000-0002-1897-3818; J.M., 0000-0002-7872-9673; B.H., 0000-0002-0432-3136; M.E., 0000-0002-2245-1668; M.K.-Z., 0000-0001-8378-8048; Y.A., 0000-0001-6156-3825; S.P.J., 0000-0002-4750-1991; P.H., 0000-0001-6486-2863; F.H.P., 0000-0003-4584-2044.

Correspondence: Philip Hogg, The Centenary Institute, Camperdown, Sydney, NSW 2050, Australia; email: phil.hogg@sydney.edu.au; and Freda H. Passam, Room 3115, Level 3E, Charles Perkins Centre, University of Sydney, John Hopkins Drive, Camperdown, Sydney, NSW 2050, Australia; email: freda.passam@sydney.edu.au.

## References

1. Chen K, Detwiler TC, Essex DW. Characterization of protein disulfide isomerase released from activated platelets. *Br J Haematol*. 1995;90(2):425-431.
2. Yadav S, Storrie B. The cellular basis of platelet secretion: emerging structure/function relationships. *Platelets*. 2017;28(2):108-118.
3. Holbrook LM, Watkins NA, Simmonds AD, Jones CI, Ouwehand WH, Gibbins JM. Platelets release novel disulfide isomerase enzymes which are recruited to the cell surface following activation. *Br J Haematol*. 2010;148(4):627-637.

4. Holbrook LM, Sasikumar P, Stanley RG, Simmonds AD, Bicknell AB, Gibbins JM. The platelet-surface disulfide isomerase enzyme ERp57 modulates platelet function. *J Thromb Haemost*. 2012;10(2):278-288.
5. Holbrook LM, Sandhar GK, Sasikumar P, et al. A humanized monoclonal antibody that inhibits platelet-surface ERp72 reveals a role for ERp72 in thrombosis. *J Thromb Haemost*. 2018;16(2):367-377.
6. Zhou J, Wu Y, Rauova L, et al. A novel role for endoplasmic reticulum protein 46 (ERp46) in platelet function and arterial thrombosis in mice. *Blood*. 2022;139(13):2050-2065.
7. Jordan PA, Stevens JM, Hubbard GP, et al. A role for the disulfide isomerase protein ERp5 in platelet function. *Blood*. 2005;105(4):1500-1507.
8. Cho J, Furie BC, Coughlin SR, Furie B. A critical role for extracellular protein disulfide isomerase during thrombus formation in mice. *J Clin Invest*. 2008;118(3):1123-1131.
9. Wu Y, Ahmad SS, Zhou J, Wang L, Cully MP, Essex DW. The disulfide isomerase ERp57 mediates platelet aggregation, hemostasis, and thrombosis. *Blood*. 2012;119(7):1737-1746.
10. Passam FH, Lin L, Gopal S, et al. Both platelet- and endothelial cell-derived ERp5 support thrombus formation in a laser-induced mouse model of thrombosis. *Blood*. 2015;125(14):2276-2285.
11. Zhou J, Wu Y, Chen F, et al. The disulfide isomerase ERp72 supports arterial thrombosis in mice. *Blood*. 2017;130(6):817-828.
12. Lu J, Holmgren A. The thioredoxin superfamily in oxidative protein folding. *Antioxid Redox Signal*. 2014;21(3):457-470.
13. Adams BM, Canniff NP, Guay KP, Hebert DN. The role of endoplasmic reticulum chaperones in protein folding and quality control. *Prog Mol Subcell Biol*. 2021;59:27-50.
14. Jang I, Pottekat A, Poothong J, et al. PDIA1/P4HB is required for efficient proinsulin maturation and ß cell health in response to diet induced obesity. *Elife*. 2019;8:e44528.
15. Li A, Song NJ, Riesenberg BP, Li Z. The emerging roles of endoplasmic reticulum stress in balancing immunity and tolerance in health and diseases: mechanisms and opportunities. *Front Immunol*. 2020;10:3154.
16. Walter P, Ron D. The unfolded protein response: from stress pathway to homeostatic regulation. *Science*. 2011;334(6059):1081-1086.
17. Morishima N, Nakanishi K. Proplatelet formation in megakaryocytes is associated with endoplasmic reticulum stress. *Genes Cells*. 2016;21(7):798-806.
18. Rendu F, Brohard-Bohn B. The platelet release reaction: granules' constituents, secretion and functions. *Platelets*. 2001;12(5):261-273 17.
19. Kim K, Hahm E, Li J, et al. Platelet protein disulfide isomerase is required for thrombus formation but not for hemostasis in mice. *Blood*. 2013;122(6):1052-1061.
20. Eletto D, Eletto D, Dersh D, Gidalevitz T, Argon Y. Protein disulfide isomerase A6 controls the decay of IRE1α signaling via disulfide-dependent association. *Mol Cell*. 2014;53(4):562-576.
21. Eletto D, Eletto D, Boyle S, Argon Y. PDIA6 regulates insulin secretion by selectively inhibiting the RIDD activity of IRE1. *FASEB J*. 2016;30(2):653-655.
22. Yang H, Wang H, Jaenisch R. Generating genetically modified mice using CRISPR/Cas-mediated genome engineering. *Nat Protoc*. 2014;9(8):1956-1968.
23. Zbidi H, Redondo PC, López JJ, Bartegi A, Salido GM, Rosado JA. Homocysteine induces caspase activation by endoplasmic reticulum stress in platelets from type 2 diabetics and healthy donors. *Thromb Haemost*. 2010;103(5):1022-1032.
24. Abdullahi A, Barayan D, Vinaik R, Diao L, Yu N, Jeschke MG. Activation of ER stress signalling increases mortality after a major trauma. *J Cell Mol Med*. 2020;24(17):9764-9773.
25. Hearn JI, Green TN, Hisey CL, et al. Deletion of Grin1 in mouse megakaryocytes reveals NMDA receptor role in platelet function and proplatelet formation. *Blood*. 2022;139(17):2673-2690.
26. Maclean JAA, Tomkins AJ, Sturgeon SA, et al. Development of a carotid artery thrombolysis stroke model in mice. *Blood Adv*. 2022;6(18):5449-5462.
27. Larsson P, Tarlac V, Wang TY, et al. Scanning laser-induced endothelial injury: a standardized and reproducible thrombosis model for intravital microscopy. *Sci Rep*. 2022;12(1):3955.
28. Ritchie ME, Phipson B, Wu D, et al. limma powers differential expression analyses for RNA-sequencing and microarray studies. *Nucleic Acids Res*. 2015;43(7):e47.
29. Wu T, Hu E, Xu S, et al. clusterProfiler 4.0: a universal enrichment tool for interpreting omics data. *Innovation (Camb)*. 2021;2(3):100141.
30. Debrincat MA, Pleines I, Lebois M, et al. BCL-2 is dispensable for thrombopoiesis and platelet survival. *Cell Death Dis*. 2015;6(4):e1721.
31. Meunier L, Usherwood YK, Chung KT, Hendershot LM. A subset of chaperones and folding enzymes form multiprotein complexes in endoplasmic reticulum to bind nascent proteins. *Mol Biol Cell*. 2002;13(12):4456-4469.
32. Kile BT. The role of apoptosis in megakaryocytes and platelets. *Br J Haematol*. 2014;165(2):217-226.
33. Toldo S, Severino A, Abbate A, Baldi A. The role of PDI as a survival factor in cardiomyocyte ischemia. *Methods Enzymol*. 2011;489:47-65.
34. Perri ER, Thomas CJ, Parakh S, Spencer DM, Atkin JD. The unfolded protein response and the role of protein disulfide isomerase in neurodegeneration. *Front Cell Dev Biol*. 2016;3:80.
35. Authi KS, Bokkala S, Patel Y, Kakkar VV, Munkonge F. Ca2+ release from platelet intracellular stores by thapsigargin and 2,5-di-(t-butyl)-1,4-benzohydroquinone: relationship to Ca2+ pools and relevance in platelet activation. *Biochem J*. 1993;294(pt 1):119-126.

36. Raturi A, Mutus B. Characterization of redox state and reductase activity of protein disulfide isomerase under different redox environments using a sensitive fluorescent assay. *Free Radic Biol Med*. 2007;43(1):62-70.

37. Májek P, Reicheltová Z, Stikarová J, Suttnar J, Sobotková A, Dyr JE. Proteome changes in platelets activated by arachidonic acid, collagen, and thrombin. *Proteome Sci*. 2010;8:56.

38. Lopez E, Bermejo N, Berna-Erro A, et al. Relationship between calcium mobilization and platelet α- and δ-granule secretion. A role for TRPC6 in thrombin-evoked δ-granule exocytosis. *Arch Biochem Biophys*. 2015;585:75-81.

39. Al-Fadhli FM, Afqi M, Sairafi MH, et al. Biallelic loss of function variant in the unfolded protein response gene PDIA6 is associated with asphyxiating thoracic dystrophy and neonatal-onset diabetes. *Clin Genet*. 2021;99(5):694-703.

40. Choi JH, Zhong X, Zhang Z, et al. Essential cell-extrinsic requirement for PDIA6 in lymphoid and myeloid development. *J Exp Med*. 2020;217(4): e20190006.

41. Di Buduo CA, Abbonante V, Marty C, et al. Defective interaction of mutant calreticulin and SOCE in megakaryocytes from patients with myeloproliferative neoplasms. *Blood*. 2020;135(2):133-144.

42. Jain K, Tyagi T, Du J, et al. Unfolded protein response differentially modulates the platelet phenotype. *Circ Res*. 2022;131(4):290-307.

43. Paul M, Kemparaju K, Girish KS. Inhibition of constitutive NF-κB activity induces platelet apoptosis via ER stress. *Biochem Biophys Res Commun*. 2017;493(4):1471-1477.

44. Kovuru N, Raghuwanshi S, Sharma DS, Dahariya S, Pallepati A, Gutti RK. Endoplasmic reticulum stress induced apoptosis and caspase activation is mediated through mitochondria during megakaryocyte differentiation. *Mitochondrion*. 2020;50:115-120.

45. Meyer BA, Doroudgar S. ER stress-induced secretion of proteins and their extracellular functions in the heart. *Cells*. 2020;9(9):2066.

46. Genereux JC, Qu S, Zhou M, et al. Unfolded protein response-induced ERdj3 secretion links ER stress to extracellular proteostasis. *EMBO J*. 2015; 34(1):4-19.

47. Spitler KM, Matsumoto T, Webb RC. Suppression of endoplasmic reticulum stress improves endothelium-dependent contractile responses in aorta of the spontaneously hypertensive rat. *Am J Physiol Heart Circ Physiol*. 2013;305(3):H344-353.

48. Coe H, Jung J, Groenendyk J, Prins D, Michalak M. ERp57 modulates STAT3 signaling from the lumen of the endoplasmic reticulum. *J Biol Chem*. 2010; 285(9):6725-6738.

49. Chiu J, Uaprasert N, Eriksson O, et al. PDI cleavage of disulfide bonds within the TP receptor inhibits signaling through Gα 13. *Blood*. 2021; 138(Supplement 1):579.

50. Reinhardt C, von Brühl ML, Manukyan D, et al. Protein disulfide isomerase acts as an injury response signal that enhances fibrin generation via tissue factor activation. *J Clin Invest*. 2008;118(3):1110-1122.

51. Zhou J, Wu Y, Wang L, et al. The C-terminal CGHC motif of protein disulfide isomerase supports thrombosis. *J Clin Invest*. 2015;125(12):4391-4406.

52. Wang L, Wu Y, Zhou J, et al. Platelet-derived ERp57 mediates platelet incorporation into a growing thrombus by regulation of the αIIbβ3 integrin. *Blood*. 2013;122(22):3642-3650.

53. Essex DW, Wu Y. Multiple protein disulfide isomerases support thrombosis. *Curr Opin Hematol*. 2018;25(5):395-402.

54. van Rooy MJ, Duim W, Ehlers R, Buys AV, Pretorius E. Platelet hyperactivity and fibrin clot structure in transient ischemic attack individuals in the presence of metabolic syndrome: a microscopy and thromboelastography study. *Cardiovasc Diabetol*. 2015;14:86.

55. Gaspar RS, Trostchansky A, Paes AM. Potential role of protein disulfide isomerase in metabolic syndrome-derived platelet hyperactivity. *Oxid Med Cell Longev*. 2016;2016:2423547.